JOURNAL OF PHYSIOLOGY AND PHARMACOLOGY 2009, 60, Suppl 4, 15-22
www.jpp.krakow.pl

S. BREZILLON[1], C. ZELTZ[1], L. SCHNEIDER[2], C. TERRYN[1], B. VUILLERMOZ[1], L. RAMONT[1,3], C. PERREAU[1], M. PLUOT[2,3], M.D. DIEBOLD[2,3], A. RADWANSKA[4], M. MALICKA-BLASZKIEWICZ[4], F.-X. MAQUART[1,3], Y. WEGROWSKI[1]

LUMICAN INHIBITS B16F1 MELANOMA CELL LUNG METASTASIS

[1]Laboratoire de Biochimie Médicale et Biologie Moléculaire, CNRS UMR 6237, IFR53 Interactions Cellules-Microenvironnement, Faculté de Médecine, Université de Reims-Champagne-Ardenne, 51095 Reims, France; [2]Laboratoire d'Anatomie Pathologique, CNRS UMR 6237, IFR53 Interactions Cellules-Microenvironnement, Université de Reims Champagne-Ardenne, 51095 Reims Cedex, France; [3]CHU de Reims, 51095 Reims Cedex, France; [4]Department of Cell Pathology, Faculty of Biotechnology, University of Wroclaw, Wroclaw, Poland

Background: Lumican is a small leucine-rich proteoglycan (SLRP) of the extracellular matrix (ECM) involved in the control of melanoma growth and invasion. The aim of the present study was to analyse the role of lumican in the regulation of the development of lung metastasis. Methods: B16F1 melanoma cells stably transfected with lumican expressing plasmid (Lum-B16F1) were injected to syngenic mice. The lung metastasis was compared to mice injected with mock-transfected B16F1 cells (Mock-B16F1). The expression of lumican, cyclin D1, apoptotic markers, vascular endothelium growth factor (VEGF) and Von Willebrand Factor (vWF) within lung metastasis nodules was investigated by immunohistochemistry. In parallel, cells cultured in presence of lumican were assayed for apoptosis and motility. Results: We observed that the number and the size of lung metastasis nodules were significantly decreased in mice injected with Lum-B16F1 cells in comparison to Mock-B16F1 cells. This was associated with an increase of tumour cell apoptosis within metastasis nodules but the cell proliferation rate remained constant in the two mice groups. In contrast, the VEGF immunostaining and the number of blood vessels within the lung metastasis nodules were decreased in the lumican-expressing tumours. *In vitro*, a significant decrease of apoptotic markers in wild type B16F1 cells incubated with increasing amounts of lumican core protein was observed. In addition, pseudotubes formation on Matrigel® and the migratory capacity of endothelial cells was inhibited by lumican. Altogether, our results indicate that lumican decreases lung metastasis development not only by inducing tumour cell apoptosis but also by inhibiting angiogenesis.

Keywords: *lung metastasis, melanoma, lumican, proteoglycan, apoptosis, angiogenesis*

INTRODUCTION

The family of small leucine-rich proteoglycans SLRPs, which includes decorin, lumican, biglycan and fibromodulin, constitutes an abundant component of the skin extracellular matrix (1). Lumican, as well as other SLRPs, is involved in collagen fibrillogenesis regulation in the dermis (2, 3) and in the cornea (4). It regulates keratocyte migration (5, 6).

Lumican expression has been reported in many types of cancer (7) including breast carcinoma (8, 9); colorectal (10, 11) and pancreatic cancer (12). It was described in stromal melanoma tissue (13) and melanoma cells (14). Its expression in cancer is believed to be related to a tumour suppressor activity. We previously demonstrated that lumican expression reduced the ability of B16F1 mouse melanoma cells to invade Matrigel® *in vitro* and to inhibit primary tumour growth by inducing melanoma cells apoptosis in syngenic mice (1). The melanoma cell migration was decreased on lumican substratum through β1 integrin (15). Moreover, lumican affects cytoskeleton organization in human melanoma A375 cells (16).

Lumican was suggested to be a major component of the ECM proteoglycans in adult human lungs. It was detected as a single component of molecular weight 65 to 90 kD (17). Immonuhistochemistry showed that lumican was mainly present in vessel walls. In lung cancer tissues, it was localized in the cytoplasm of cancer cells and/or stromal tissues adjacent to cancer cells (9).

Anti-angiogenic and pro-apoptotic drugs have been developed to inhibit lung cancer progression (18). The *in vivo* anti-cancer effect of these drugs was associated with a decreased microvessel density as well as a reduction of tumour cell proliferation and increased tumour cell apoptosis. In avian embryo model, gene expression profiling of the angiogenic switch in experimental glioma suggested that lumican could be a potential regulator of the invasive process (19). Transcriptome analysis of endothelial cell gene expression identified lumican as a novel regulator of angiogenesis. Lumican was described to inhibit endothelial cell activation of p38 mitogen-activated protein kinase (p38 MAPK), as well as their invasion, angiogenic sprouting, and vessel formation in mice (20).

Since lumican was suggested to be a major component of the proteoglycan matrix in healthy adult human lungs (17), we investigated whether human recombinant lumican was able to decrease the number and the size of lung metastasis and to study

the mechanism of its action. Using lumican-expressing B16F1 melanoma cells injected in the tail vein of mice, we demonstrated that lumican decreased the number and the size of lung metastasis nodules by inducing tumour cell apoptosis and inhibited the release of VEGF, therefore decreasing the density of blood vessels in the lung metastasis nodules. *In vitro*, using human umbilical vein endothelial cells (HUVEC), we demonstrated that lumican inhibited endothelial cell tube formation and endothelial cell migration. Therefore, we suggest that lumican might be a powerful and effective anti-tumour agent against melanoma, due to its inhibition of both primary tumour growth and metastatic spreading to the lungs, associated with a pro-apoptotic and angiostatic effect.

MATERIALS AND METHODS

Reagents and antibodies

Recombinant human lumican core protein was produced as previously described (1). Type I Collagen was prepared from rat tail tendon by extraction with 0.1 M acetic acid (21). Human plasma fibronectin and propidium iodide were obtained from AbCys (Paris, France). Hoechst^{33342} was obtained from Invitrogen (Cergy-Pontoise, France). Doxorubicin was obtained from Pharmacia and UpJohn (St Quentin en Yvelines, France). Matrigel® (ECM gel) was purchased from BD Biosciences (Bedford, MA, USA). VEGF and basic Fibroblast Growth Factor (bFGF) were purchased from Sigma-Aldrich (St Louis, MO, USA).

The following rabbit polyclonal primary antibodies were used: anti-human actin (A5060, Sigma), anti-human lumican (1); anti-human caspase-3, anti-human cleaved caspase-3 (Cell Signaling Technology, Danvers, MA, USA). Anti-human vWF was provided by Millipore (Molsheim, France). Rabbit polyclonal antibody anti-mouse Cyclin D1 (SP4) was obtained from Labvision (Westinghouse, CA, USA).

The following mouse monoclonal primary antibody were used: anti-human poly (ADP-ribose) polymerase (PARP), anti-human cleaved PARP (Cell Signaling Technology), anti-human VEGF (Santa Cruz Biotechnology, CA, USA). Mouse isotype control IgG1,κ fraction (MOPC-21) (Sigma®, Saint-Quentin Fallavier, France).

Cells and cell culture

B16F1 cells, a lung metastatic subline of murine B16 melanoma, were kindly provided by Dr M. Gregoire (INSERM UMRS 419, Nantes, France). They were cultured in RPMI-1640 medium supplemented with 5% Fetal Bovine Serum (FBS). Mock-transfected B16F1 cells (Mock-B16F1, transfected with pcDNA3 vector) and HLum-transfected B16F1 cells (Lum-B16F1, transfected by pcDNA3-HLum construct) were cultured as already described (1). HUVEC were purchased from PromoCell (Heidelberg, Germany) and were cultured in Endothelial Cell Growth Medium (ECGM PromoCell), supplemented with 0.4% (w/v) endothelial cell growth supplement/heparin, 5% (v/v) FBS, 10 ng/ml Epidermal Growth Factor (EGF), 1 µg/ml hydrocortisone, and 50 ng/ml amphotericin B. The medium was supplemented with VEGF or bFGF (15 ng/ml).

Matrigel® (BD Biosciences) (10 mg/ml), mixed or not with lumican (10 µg/ml in 18 mM acetic acid), was added to a 24-well plate, (Nunc, Roskilde, Denmark), (300 µl per well). After 30 min of incubation at 37°C, 5x 10^4 HUVEC cells were suspended either in a serum free endothelial cell growth medium or in the same medium supplemented with either bFGF (15 ng/ml) or VEGF (15 ng/ml) and then seeded onto the gel. Pseudotube formation was observed after 24h.

Animals

Female C57BL/6 mice were purchased from Harlan-France (Gannat, France). Animals were individually caged in a room with constant temperature and humidity, standard food and water ad libitum. All mice were acclimatized for one week before starting the experiments. The experiments were conducted according to the recommendations of the Centre National de la Recherche Scientifique. At day 0, 10^5 B16F1 melanoma cells were injected in the tail vein of mice (n=5 for each group). At day 14th, mice were sacrified and lungs collected for histological examination.

Histological stainings

Mice lung sections (5 µm) were stained with standard Hematoxyline Phloxin Safran solution (HPS). Masson's Trichrome staining was also performed to visualize collagen fibres and blood vessels.

Immunohistochemistry

Tissue samples were fixed with 4% fresh paraformaldehyde in phosphate buffered saline (PBS), pH 7.2 at 4°C overnight. Serial sections (5 µm) of paraffin-embedded samples were processed for immunohistochemical studies as already described (1). After deparaffinisation, the sections were treated with 0.3% H_2O_2 for 10 min at room temperature to block endogenous peroxidase. The slides were heated in a pressure cooking in 10 mM sodium citrate buffer (pH 6.0), then washed in PBS and incubated with normal serum from the Vectastain® Universal Quick kit (Vector Laboratories, Burlingame, CA, USA) for 20 min at room temperature to block non specific binding. Then, the sections were incubated with the indicated primary antibodies at 4°C overnight. After washing with PBS, the slides were treated for 1 h at room temperature with the secondary antibody, either goat anti-rabbit (Vector Laboratories) or goat anti-mouse immunoglobulin (Vector Laboratories), depending on the primary antibody used. All secondary antibodies were peroxidase-labelled and stained with 3-amino-9-ethylcarbazole (Vector Laboratories). Counterstaining was performed with Harris hematoxyline.

Western immunoblotting

Increasing concentrations of human lumican core protein, (0, 10, 50 µg/ml), were added to the B16F1 cell culture medium for sixteen hours. Cells were harvested by scrapping and subjected to protein extraction as already described (1). The protein concentration was determined by Bradford method (22). Following electrophoresis, proteins were transferred from polyacrylamide gels to nitrocellulose by electroblotting. The membranes were soaked in TBS-T solution (0.005% Tween 20, 20 mM Tris and 140 mM NaCl, pH 7.6) containing 5% BSA for 2 h. After washing, the membranes were incubated with primary antibodies at a final dilution of 1:1000 overnight at 4°C. The membranes were washed with TBS-T and probed with a 1:10000 dilution of a goat anti-rabbit secondary antibody conjugated to horseradish peroxidase in a solution of 1% BSA in TBS-T for 30 min at room temperature. After washing in TBS-T, the bands were revealed by the ECL Plus Chemiluminescence Detection kit (GE Healthcare, Little Chalfont, UK).

Cell migration quantification using time-lapse microscopy

HUVEC cells were seeded on uncoated, type-I collagen-coated or lumican-coated wells (120 µg per well in 12-well plates in 2 ml/well containing 5000 cells). Twenty four h after

seeding, cell motility analysis was performed using an inverted microscope (Axiovert 200M; Zeiss, Oberkoken, Germany) equipped with a small transparent environmental chamber (Climabox; Zeiss) with 5% (v/v) CO_2 in air at 37°C. The microscope was driven by the Metamorph software (Roper Scientific, Evry, France), and images were recorded with a charge-coupled device camera (CoolsnapHQ; Roger Scientific). Cell migration was characterized and quantified using an interactive tracking method as already described (23).

For each individual cell, on each substratum, the following parameters of cell locomotion were studied: (i) the average migration speed of a single cell (µm/h) including the stationary phases or breaks in which the cell is not motile; (ii) the frequency of breaks (number/4h) and their mean length (min); and (iii) the velocity (µm/h) which represents for each cell its period of actual movement excluding breaks (24).

Image analysis

The mean surface of lung metastasis nodules was calculated from 7 different sections for each nodule by image analysis using ImageJ software (25). VEGF staining in lung metastasis nodules sections was quantified from the pictures by ImageJ software. The mean number of blood vessels was analysed from vWF-positive endothelial cells staining after retrieval of the melanin pigment background by threshold ingeneering with ImageJ software (NIH). The network of the capillary pseudotubes formed after 24 h by HUVEC seeded on Matrigel® was quantified by computer analysis ImageJ software and NeuronJ plug-in tool (25).

Statistical analysis

Results were expressed as mean ± standard deviation. For *in vitro* experiments, statistical significance between groups was assessed by unpaired Student's *t* test. Differences with $P<0.01$ were considered significant. Statistical analysis of morphological data of lung metastasis nodules sections was performed using the non-parametric Mann-Withney *U* rank sum test. The *P* value < 0.05 was considered statistically significant.

RESULTS

Lumican inhibits lung metastasis development

B16F1 melanoma cells injected in the mouse tail vein two weeks later developed lung metastasis nodules (*Fig. 1*). The mean number of lung metastasis nodules was significantly ($P<0.001$) decreased in mice injected with Lum-B16F1 cells compared to mice injected with Mock-B16F1 cells (*Fig. 1C*). Immunohistochemistry analysis showed that, in comparison to Mock-B16F1 cells (*Fig. 1D*), lumican was overexpressed in the metastatic nodules obtained with Lum-B16F1 cells (*Fig. 1E*). *Fig. 2.* shows Masson's Trichrome stainings of representative lung metastasis from a Mock-B16F1 cells-injected mouse (*Fig. 2A* a-e) and a Lum-B16F1 cells-injected mouse (*Fig. 2B* a-d). The metastatic nodules were characterized by numerous melanin-positive B16F1 cells surrounding pre-existing blood vessels or bronchial epithelia. Small blood vessels and capillaries were

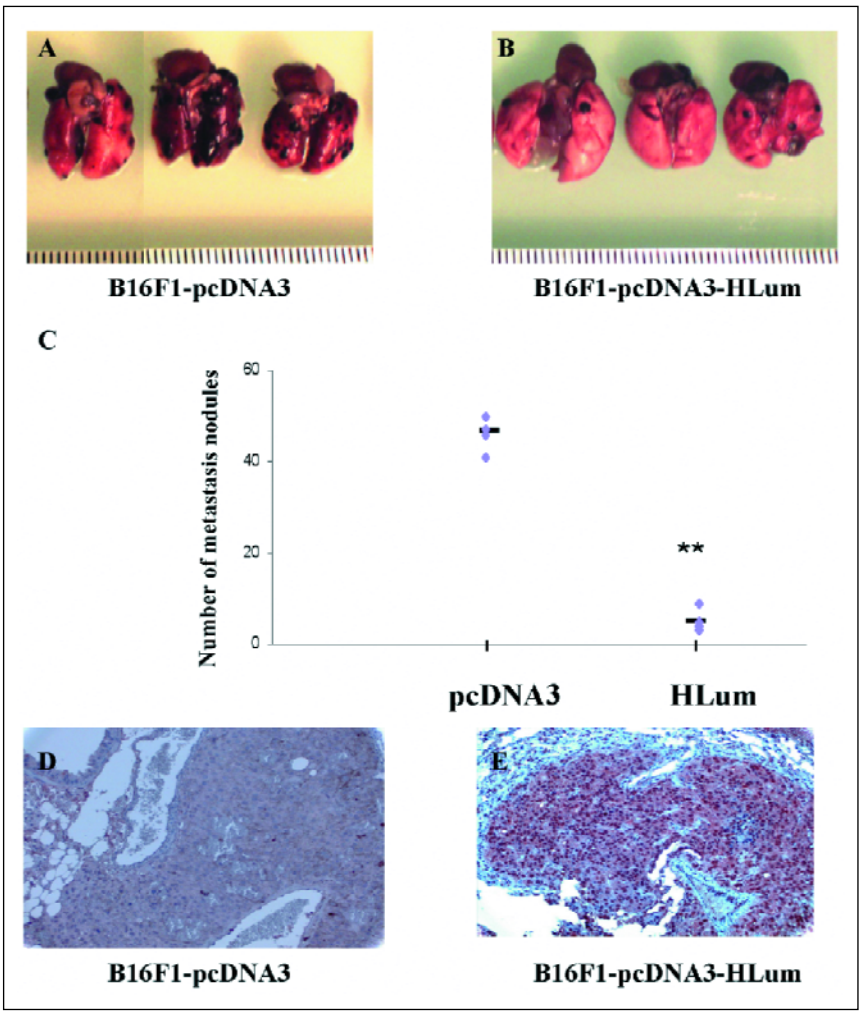

Fig.1. The influence of lumican on the formation of lung metastasis nodules.
Lung metastasis nodules were obtained after injection of 10^5 mock-transfected (Mock-B16F1) (A) or HLum-transfected (Lum-B16F1) (B) B16F1 cells in the tail vein of syngenic C57BL6 mice, as described in Material and Methods. Lungs were collected at day 14th and the number of lung metastasis nodules was counted in each mice group (C). The bars represent median values. ** : $P<0.001$. The immunohistochemical staining of lumican expressed in mock-B16F1 (D) and Lum-B16F1 cells (E). Magnification X20 (D,E).

visible inside the nodules. Necrotic plaques could be observed in the Lum-B16F1 cells mice group (*Fig. 2B* a). Large variations in the number and in the size of the nodules within one section but also within one mice group were observed.

To better characterize the lung metastasis nodules of each mice group, the mean number and the mean surface of lung metastasis nodules were measured (*Fig. 2C*). The mean surface of the nodules was significantly lower ($P<0.05$) in the lumican-overexpressing mice group ($5.3 \times 10^6 \pm 3.0 \times 10^6$) in comparison to the control mice group ($13.3 \times 10^6 \pm 10.8 \times 10^6$), although large variations from one mouse to another within the same group was observed. Therefore, the microscopic results confirmed the macroscopic observations and suggested that overexpression of lumican might inhibit lung metastasis development.

Lumican induces B16F1 melanoma cell apoptosis in lung metastasis nodules

The proliferation of B16F1 melanoma cells within the nodules was investigated by immunohistochemistry with an antibody raised against cyclin D1 (*Fig. 3A, B*). The percentage of cyclin D1-positive nuclei was similar in both types of B16F1 cells independently of their lumican expression (34.1±15.0 and 38.8±14.4, respectively). Therefore, lumican expression seemed to have no significant effect on the proliferation of B16F1 melanoma cells within the nodules. The apoptosis of B16F1 was then investigated by immunohistochemistry on lung metastasis nodule sections with antibodies raised against apoptosis cell markers: cleaved caspase 3 and cleaved PARP. In contrast to Mock-B16F1 cells (*Fig. 3C*, *E*), metastasis nodules of Lum-B16F1 cells exhibited cleaved caspase 3 and cleaved PARP stainings in the cytoplasm and in the nucleus, respectively (*Fig. 3D, F*).

In order to confirm the pro-apoptotic effect of lumican overexpression, wild type B16F1 melanoma cells were incubated *in vitro* in the presence of increasing concentrations, (0, 10, 50 µg/ml), of recombinant human lumican core protein for sixteen hours. The expression of total caspase 3 and cleaved PARP was then analysed by Western immunoblotting from whole cell extract (*Fig. 4*). Noticeably, total caspase 3 expression was down-regulated in the presence of increasing concentrations of lumican while, concomitantly, cleaved PARP expression was up-regulated, confirming a pro-apoptotic effect of lumican on B16F1 cells.

These results suggest that lumican inhibits lung metastasis nodule growth by inducing tumour cell apoptosis within the metastatic nodules.

Lumican expression decreases VEGF expression and blood vessels density in lung metastasis nodules

VEGF expression in lung metastasis nodules was analysed by immunohistochemistry (*Fig. 5A, B*). The intensity of the staining

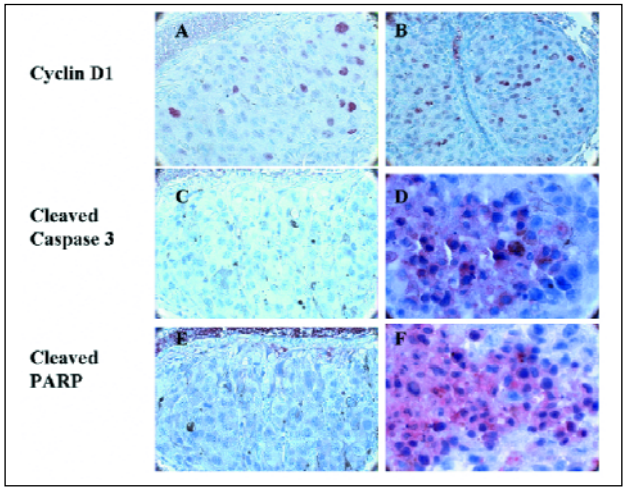

Fig. 3. Lumican induces B16F1 cells apoptosis in mouse lung metastasis nodules. Lung metastasis nodules from Mock-B16F1 cells (A,C,E) or from Lum-B16F1 cells (B,D,F) were obtained as described. Immunohistochemistry was performed on lung metastasis nodule sections with antibodies directed against cyclin D1 (A,B), cleaved caspase 3 (C,D) and cleaved PARP (E,F). Magnification X40 (A-C, E), X100 (D,F).

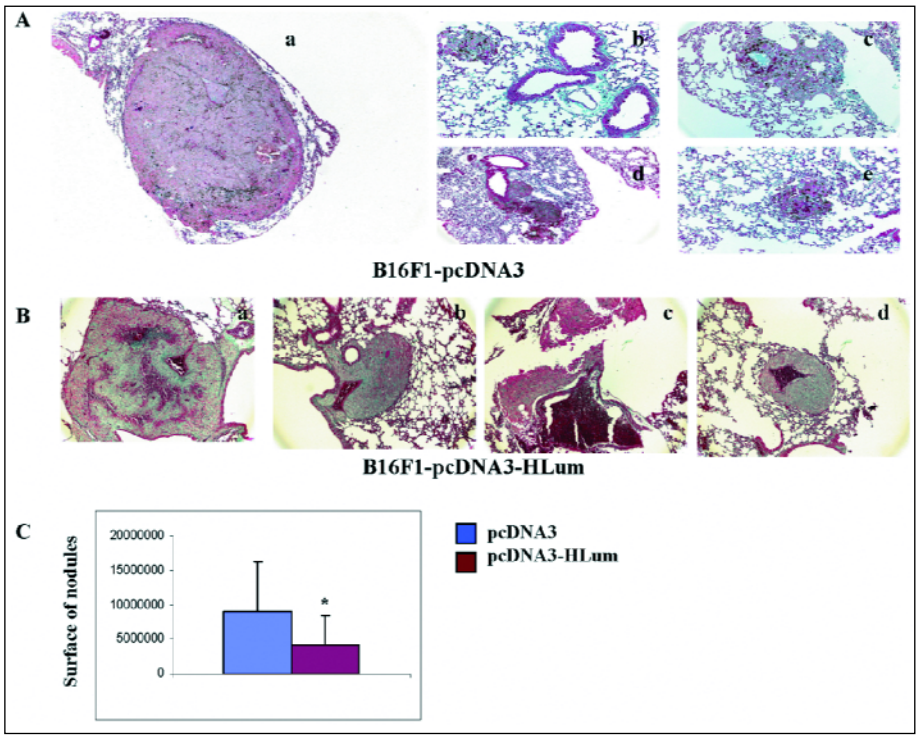

Fig. 2. Inhibition by lumican of the size of lung metastasis nodules observed after Masson's Trichrome staining of the sections.
Lung metastasis nodules were obtained as described in *Fig. 1*. Standard Masson's Trichrome staining was performed on lung metastasis nodule sections. A representative series of nodules from one section of Mock-B16F1 cells mouse is illustrated (A a-e). The histology of the nodules was characterized by numerous melanin positive B16F1 cells surrounding pre-existing blood vessels and/or bronchial epithelia (A c,d). Small blood vessels and capillaries were visible inside the nodules. A representative series of nodules from one section of one Lum-B16F1 cells mouse is illustrated (B a-d). The mean size of lung metastasis nodules (± SD) is shown in the diagram (C). * : $P<0.05$. Magnification X5 (A a), X10 (A d; Ba-d), X20 (A b,c,e).

was quantified by image analysis software in each mice group as shown in the upper right diagram. In comparison to Mock-B16F1 cells (*Fig. 5A*), Lum-B16F1 cells nodules (*Fig. 5B*) exhibited significantly lower ($P<0.05$) expression of VEGF. This result led us to investigate the density of the blood vessels network within the nodules of the lung metastasis of each mice group. Blood vessels were visualized using an antibody directed against vWF, a marker of endothelial cells (*Fig. 5C, D*) and the number of blood vessels within the nodules was counted, as shown in the lower right diagram. A significant ($P<0.05$) decrease of the mean number of blood vessels was observed in the metastasis nodules of Lum-B16F1 cells compared to the Mock-B16F1 cells control nodules. This result suggested that lumican might inhibit neo-angiogenesis in the metastasis nodules.

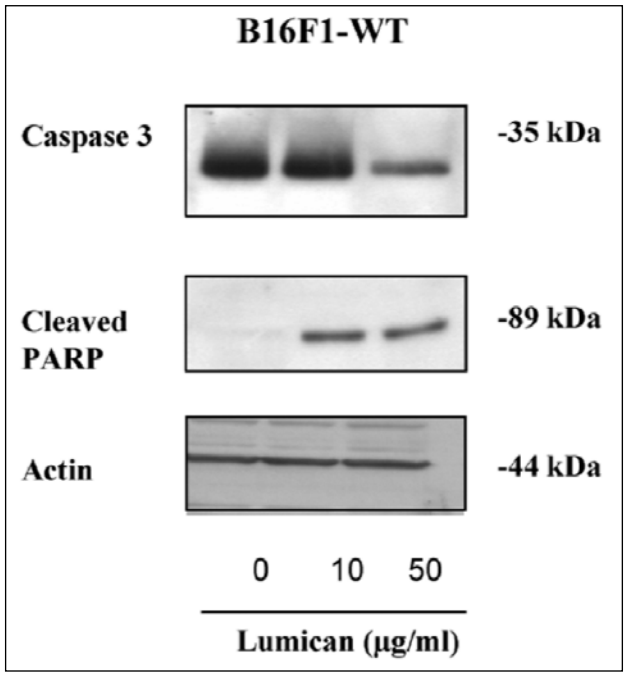

Fig. 4. Effect of lumican on total caspase 3 and cleaved PARP expression in wild type B16F1 cells.
Increasing concentrations of human lumican core protein, as described below the blots, were added to the cell culture medium for sixteen hours. Cells were collected, proteins extracted and subjected to Western immunoblotting as described in Materials and Methods. The migration position of the Mr 35,000-caspase 3, 89,000-cleaved PARP and 44,000-actin bands are indicated.

Lumican inhibits pseudotube formation in vitro

The ability of HUVEC to form pseudotubes on Matrigel® *in vitro* (*Fig. 6A, B*) was studied after addition of 10 µg/ml of recombinant lumican core protein within the gel (*Fig. 6B*). Twenty four hours after seeding, the presence of lumican within Matrigel® impaired pseudotube formation by the endothelial cells (*Fig. 6B*). The inhibitory effect of lumican in the endothelial basal cell medium was abolished by the presence of bFGF (15 ng/ml) or VEGF (15 ng/ml) (data not shown). These *in vitro* results confirmed the angiostatic effects of lumican previously observed *in vivo*.

Lumican inhibits in vitro endothelial cell migration

The proliferation of endothelial cells was investigated by immunohistochemistry with an antibody raised against cyclin D1 (data not shown). The percentage of positive cyclin D1 nuclei in endothelial cells was not significantly affected by lumican coating compared to controls (16.4±4 and 17.5±3, respectively). Therefore, lumican had no significant effect on the proliferation of endothelial cells. The apoptosis of endothelial cells was then investigated by Hoechst labelling. The percentage of endothelial cells with moon shape nuclei or condensed chromatin was very low (3%) and was not affected by the presence of lumican. The absence of effect of lumican on HUVEC cell proliferation and apoptosis led us to study the effects of lumican on endothelial cell migration. Continuous single cell tracking permitted to visualize the trajectories of cells grown on plastic, type I collagen, or lumican coatings. In contrast to uncoated surfaces (*Fig. 7A*) or type I collagen (*Fig. 7B*), lumican drastically decreased the trajectory of endothelial cells (*Fig. 7C*). On plastic or type I collagen, cells moved along a more linear path or a more winding path, while cells cultured on lumican exhibited shorter or circular trajectories around their starting points (*Fig. 7A*). The migration speed of endothelial cells on plastic or on type I collagen was 28 % higher ($P<0.01\%$) than on lumican (*Fig. 7D*). In addition to the migration speed (µm/h) which denotes the average speed of a single cell over the whole observation time, the stationary phases or breaks

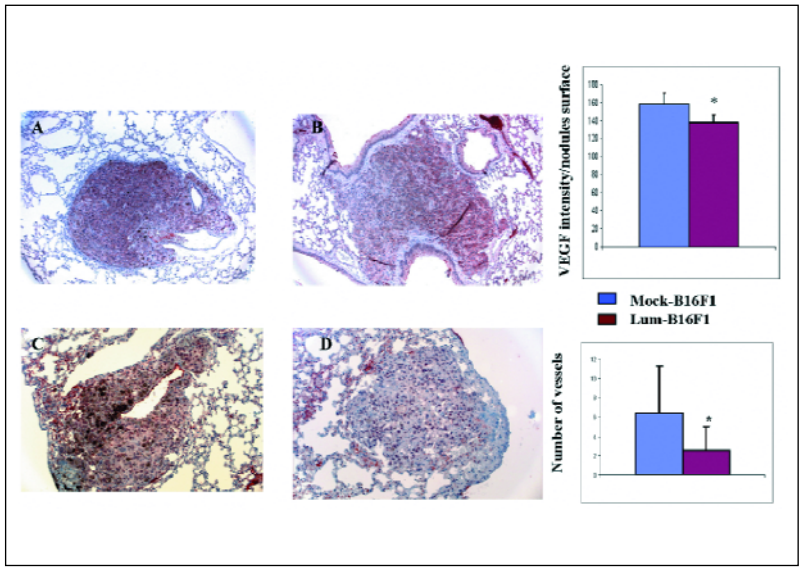

Fig. 5. Lumican inhibits VEGF expression and decreases blood vessels density in lung metastasis nodules.
Representative stainings of lung metastasis nodules from Mock-B16F1 cells (A,C) and from Lum-B16F1 cells (B,D). Immunohistochemistry was performed on lung metastasis nodules sections with antibodies directed against VEGF (A,B). VEGF staining was detected in nodules obtained with Mock-B16F1 cells and Lum-B16F1 cells. The quantification of the intensity of the staining by image analysis is shown in the upper right diagram. * : $P<0.05$.
Blood vessels were labelled using an antibody directed against vWF, a specific marker of endothelial cells (C,D). The number of blood vessels within the nodules was counted by image analysis. Results are shown in the lower right diagram. * : $P<0.05$. Magnification X10 (A,B), X20 (C,D).

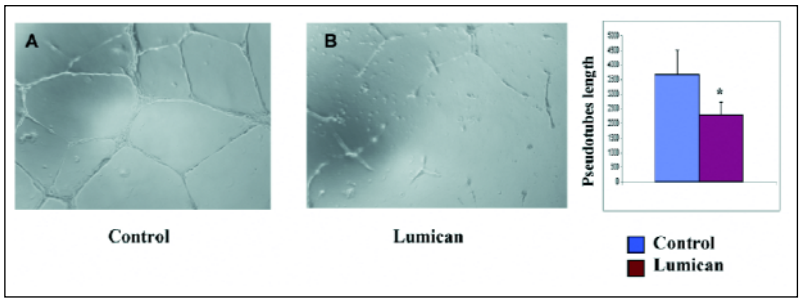

Fig. 6. Lumican inhibits *in vitro* pseudotube formation by endothelial cells.
Pseudotube formation on Matrigel® (A) or Matrigel® ECM gel mixed with 10 µg/ml of lumican (B) was observed twenty four hours after HUVEC seeding. Magnification X40. The semi-quantitative evaluation of the pseudotube network was performed using ImageJ software and NeuronJ plugin and is shown in the diagram.* : $P<0.05$.

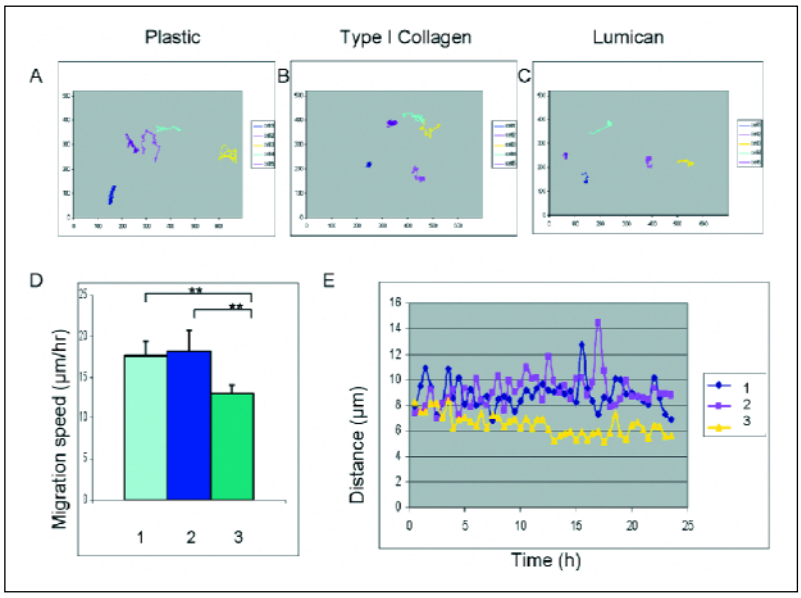

Fig. 7. Lumican inhibits endothelial cell migration.
Cells were plated on a 12-well plate at 5000 cells per well. The migration of individual living cells was determined by means of computer-assisted phase contrast videomicroscopy during 24 hours as described in Materials and Methods. Frames (A), (B), and (C) illustrate the trajectories of endothelial cells cultured on plastic or type I collagen- or lumican- coated surfaces. Frame (D) shows the mean migration speed of endothelial cell population cultured on plastic (1) or type I collagen- coated (2) or lumican- coated (3) surfaces. Frame (E) represents the distance of migration every 30 min for 24h. No break was detected whatever the nature of the substratum. The graph shows the mean values of three independent experiments. (15 cells were analysed per substratum). ** : $P< 0.01$.

(frequence and length), in which the cell is not motile, and the velocity (µm/h) which represents for each cell its period of actual movement excluding breaks, were analysed (24). As shown in *Fig. 7E*, which represents the distance of migration every 30 min for 24 h, no break was detected whatever the nature of the substratum. The migration of endothelial cells was 25 % higher on a collagen matrix or on plastic than on lumican ($P<0.05$).

Altogether, these results indicate that lumican inhibits lung metastasis nodules growth not only by inducing melanoma cell apoptosis but also by inhibiting endothelial cell migration and therefore angiogenesis within the lung metastasis nodules.

DISCUSSION

In this study, we showed that lumican the ECM protein, decreased experimental lung metastasis development in mice by increasing tumour cell apoptosis, by decreasing VEGF expression and by decreasing the neovascularization.

The development of tumour metastasis is a multistep process. Key step of this process is the interaction of tumour cells with the extracellular matrix macromolecules. On the other hand, ECM influences the behaviour of tumour cells. We previously demonstrated that recombinant human lumican inhibited the development of B16F1 primary tumours in mice by inducing tumour cell apoptosis (1). This effect was characterized by an increase of cell adhesion mediated by β1 integrin expression and an inhibition of the migration of melanoma cells (15). The apoptosis in lumican-expressed tumour nodules was characterized by enhanced immunostaining of cleaved PARP and cleaved caspase 3. *In vitro*, a significant decrease of caspase 3 expression and an increased expression of cleaved PARP in wild type B16F1 cells incubated with increasing amounts of lumican core protein were observed without alteration of the proliferation rate. Pro-apoptotic effect of lumican was already described in cornea (26-28) and in primary tumours containing melanoma cells (1). Data from Goldoni *et al.* suggest a role for decorin, another member of the SLRP family, as a powerful and effective therapeutic agent against breast cancer due to its inhibition of both primary tumour growth and metastatic spreading to the lungs associated with a pro-apoptotic effect (29, 30). In our study, apoptotic melanoma effect was not observed in the control mice group.

In contrast, the VEGF immunostaining and the number of blood vessels within the lung metastasis nodules were decreased in the lumican-expressing nodules. *In vitro*, pseudotube formation on Matrigel® by human endothelial cells (HUVEC) was inhibited by lumican. Moreover, in comparison to type I collagen coating or plastic, lumican coating induced a significant alteration of the endothelial cell trajectory and a decrease of their migration speed. B16F1 cells induce angiogenesis in metastatic nodules by stimulation of VEGF expression in distant organs. Angiogenic capacity of metastatic B16F1 cells has been widely described (31, 32). B16F1 cells metastatic potential can be increased by their enhanced release of bFGF and VEGF after phorbol ester treatment (33). Compared to mock-transfected B16F1 cells, a significant decrease of the mean number of blood vessels was observed in lung metastatic nodules developed from lumican-transfected B16F1 cells. Thus, the inhibition of the metastatic spreading to the lungs might also depend on the anti-angiogenic properties of lumican (19, 20, 34). It must be pointed out that decorin, another

member of the SLRP family, was also described to suppress tumour cell-mediated angiogenesis (35). Decorin was shown to inhibit endothelial cell migration by interfering with VEGF-stimulated NO release (36-38). In our study, the VEGF staining intensity was significantly decreased in the nodules obtained with lumican-transfected cells. This decreased VEGF expression may contribute to the decreased nodule vascularization that we observed. It will be interesting to assess if lumican inhibits the angiogenesis in another type of tumours (39-41). Moreover, the decreased vascularization might depend on a direct inhibition of neoangiogenesis by lumican, as suggested by its capacity to inhibit *in vitro* pseudotube formation by endothelial cells. Albig and collaborators (20), monitered the effects of recombinant lumican on human microvascular endothelial cells (HMEC) and HUVEC. Recombinant lumican significantly diminished the activation of p38 MAPK in response to VEGF or bFGF in HMEC cells. In that study, lumican inhibited the invasive capacities of HMEC only, whereas HUVEC appeared insensitive to its angiostatic activity. These observations suggest that lumican mediates angiostasis in an endothelial cell- and context- specific manner, confirming the observation that lumican inhibited angiogenic sprouting of HUVEC cells was unefficient after treatment with VEGF or bFGF.

Lumican was able to inhibit pseudotube formation in Matrigel® without affecting endothelial cell apoptosis and/or proliferation. Therefore, we investigated whether lumican could interfere with the motility of endothelial cells. For that purpose, HUVEC were tracked by videomicroscopy for 24 h on glass coverslips or on type I collagen coating, or lumican coating. The trajectory of endothelial cells was completely different in the presence of lumican compared to glass or collagen substratum. Cell mobility was poor on lumican coating, most of the cells making shorter or circular trajectories around their starting points. Their mean speed was also significantly decreased. These results show that the endothelial cell migration is strongly decreased in the presence of lumican. We recently showed that melanoma cell migration was also inhibited by lumican. This inhibition was correlated with altered cytoskeleton network (16). The inhibition of the migration of endothelial cells in presence of lumican might also be involved in angiostatic activity. Similar activity was previously described for decorin (36, 37, 42-46) and for the NC1 domain of type XIX collagen (47).

Taken together, our data demonstrate that lumican expression inhibits the formation of lung metastatic nodules in a mouse experimental model of melanoma. This effect seems to be due to a pro-apoptotic effect on tumour cells and to an inhibition of tumour neoangiogenesis in the metastasis nodules. Further investigations will be necessary to analyse the signalling pathway and the molecular mechanisms by which lumican exerts its angiogenic activities within normal and diseased vascular microenvironments.

Acknowledgement: The financial support of the Institut National du Cancer (ACi 2007-2009 Canceropôle Grand-Est), FEDER (CPER 2007) Region Champagne-Ardenne, and the Ligue Nationale contre le Cancer (comite de la Marne) is gratefully acknowledged. Dr Vuillermoz present addres is: iDD Biotech, 62572 Dardilly, France.

Conflict of interests: None declared.

REFERENCES

1. Vuillermoz B, Khoruzhenko A, D'Onofrio MF, *et al.* The small leucine-rich proteoglycan lumican inhibits melanoma progression. *Exp Cell Res* 2004; 296: 294-306.
2. Iozzo RV. The family of the small leucine-rich proteoglycans: key regulators of matrix assembly and cellular growth. *Crit Rev Biochem Mol Biol* 1997; 32: 141-174.
3. Chakravarti S, Magnuson T, Lass JH, Jepsen KJ, LaMantia C, Carroll H. Lumican regulates collagen fibril assembly: skin fragility and corneal opacity in the absence of lumican. *J Cell Biol* 1998; 141: 1277-1286.
4. Cornuet PK, Blochberger TC, Hassell JR. Molecular polymorphism of lumican during corneal development. *Invest Ophthalmol Vis Sci* 1994; 35: 3: 870-877.
5. Yeh LK, Chen WL, Li W, *et al.* Soluble lumican glycoprotein purified from human amniotic membrane promotes corneal epithelial wound healing. *Invest Ophthalmol Vis Sci* 2005; 46: 479-486.
6. Seomun Y, Joo CK. Lumican induces human corneal epithelial cell migration and integrin expression via ERK 1/2 signaling. *Biochem Biophys Res Commun* 2008; 372: 221-225.
7. Naito Z. Role of the small leucine-rich proteoglycan (SLRP) family in pathological lesions and cancer cell growth. *J Nippon Med Sch* 2005; 72: 137-145.
8. Leygue E, Snell L, Dotzlaw H, *et al.* Lumican and decorin are differentially expressed in human breast carcinoma. *J Pathol* 2000; 192: 313-320.
9. Matsuda Y, Yamamoto T, Kudo M, *et al.* Expression and roles of lumican in lung adenocarcinoma and squamous cell carcinoma. *Int J Oncol* 2008; 33: 1177-1185.
10. Lu YP, Ishiwata T, Kawahara K, *et al.* Expression of lumican in human colorectal cancer cells. *Pathol Int* 2002; 52: 519-526.
11. Seya T, Tanaka N, Shinji S, *et al.* Lumican expression in advanced colorectal cancer with nodal metastasis correlates with poor prognosis. *Oncol Rep* 2006; 16: 1225-1230.
12. Koninger J, Giese T, di Mola FF, *et al.* Pancreatic tumor cells influence the composition of the extracellular matrix. *Biochem Biophys Res Commun* 2004; 322: 943-949.
13. Brezillon S, Venteo L, Ramont L, *et al.* Expression of lumican, a small leucine-rich proteoglycan with antitumour activity, in human malignant melanoma. *Clin Exp Dermatol* 2007; 32: 405-416.
14. Sifaki M, Assouti M, Nikitovic D, Krasagakis K, Karamanos NK, Tzanakakis GN. Lumican, a small leucine-rich proteoglycan substituted with keratan sulfate chains is expressed and secreted by human melanoma cells and not normal melanocytes. *IUBMB Life* 2006; 58: 606-610.
15. D'Onofrio MF, Brezillon S, Baranek T, *et al.* Identification of beta1 integrin as mediator of melanoma cell adhesion to lumican. *Biochem Biophys Res Commun* 2008; 365: 2: 266-272.
16. Radwanska A, Baczynska D, Nowak D, *et al.* Lumican affects actin cytoskeletal organization in human melanoma A375 cells. *Life Sci* 2008; 83: 651-660.
17. Dolhnikoff M, Morin J, Roughley PJ, Ludwig MS. Expression of lumican in human lungs. *Am J Respir Cell Mol Biol* 1998; 19: 582-587.
18. Lee HJ, Lee HJ, Song GY, *et al.* 6-(1-Oxobutyl)-5,8-dimethoxy-1,4-naphthoquinone inhibits lewis lung cancer by antiangiogenesis and apoptosis. *Int J Cancer* 2007; 120: 2481-2490.
19. Hagedorn M, Javerzat S, Gilges D, *et al.* Accessing key steps of human tumor progression *in vivo* by using an avian embryo model. *Proc Natl Acad Sci USA* 2005; 102: 1643-1648.
20. Albig AR, Roy TG, Becenti DJ, Schiemann WP. Transcriptome analysis of endothelial cell gene expression induced by growth on matrigel matrices: identification and characterization of MAGP-2 and lumican as novel regulators of angiogenesis. *Angiogenesis* 2007; 10: 197-216.

21. Piez KA. The amino acid chemistry of some calcified tissues. *Ann N Y Acad Sci* 1963; 109: 256-268.
22. Bradford MM. A rapid and sensitive method for the quantitation of microgram quantities of protein utilizing the principle of protein-dye binding. *Anal Biochem* 1976; 72: 248-254.
23. Zahm JM, Kaplan H, Herard AL, *et al.* Cell migration and proliferation during the in vitro wound repair of the respiratory epithelium. *Cell Motil Cytoskeleton* 1997; 37: 33-43.
24. Fourre N, Millerot-Serrurot E, Garnotel R, *et al.* Extracellular matrix proteins protect human HT1080 cells against the antimigratory effect of doxorubicin. *Cancer Sci* 2008; 99: 1699-1705.
25. Meijering E, Jacob M, Sarria JC, Steiner P, Hirling H, Unser M. Design and validation of a tool for neurite tracing and analysis in fluorescence microscopy images. *Cytometry A* 2004; 58: 167-176.
26. Vij N, Roberts L, Joyce S, Chakravarti S. Lumican suppresses cell proliferation and aids Fas-Fas ligand mediated apoptosis: implications in the cornea. *Exp Eye Res* 2004; 78: 957-971.
27. Chakravarti S. Functions of lumican and fibromodulin: lessons from knockout mice. *Glycoconj J* 2002; 19: 287-293.
28. Nagata S, Golstein P. The Fas death factor. *Science* 1995; 267(5203): 1449-1456.
29. Goldoni S, Iozzo RV. Tumor microenvironment: modulation by decorin and related molecules harboring leucine-rich tandem motifs. *Int J Cancer* 2008; 123: 2473-2479.
30. Goldoni S, Seidler DG, Heath J, *et al.* An antimetastatic role for decorin in breast cancer. *Am J Pathol* 2008; 173: 844-855.
31. Berston ED, Ramos DM, Kramer RH. Metastatic melanoma cells interact with the reticular fibres of the lymph node. *Melanoma Res* 1994; 4: 115-125.
32. La Porta CA, Di Dio A, Comolli R. Inhibition of PKCalpha decreases the gelatinase activity and the angiogenic and metastatic ability of the highly metastatic B16 murine melanoma cells. *Angiogenesis* 1999; 3 241-247.
33. La Porta CA, Comolli R. Angiogenic capacity and lung-colonizing potential in vivo is increased in weakly metastatic B16F1 cells and decreased in highly metastatic BL6 cells by phorbol esters. *Clin Exp Metastasis* 1998; 16: 399-405.
34. Schaefer L, Raslik I, Grone HJ, *et al.* Small proteoglycans in human diabetic nephropathy: discrepancy between glomerular expression and protein accumulation of decorin, biglycan, lumican, and fibromodulin. *FASEB J* 2001; 559-561.
35. Grant DS, Yenisey C, Rose RW, Tootell M, Santra M, Iozzo RV. Decorin suppresses tumor cell-mediated angiogenesis. *Oncogene* 2002; 21: 4765-4777.
36. Fan H, Sulochana KN, Chong YS, Ge R. Decorin derived antiangiogenic peptide LRR5 inhibits endothelial cell migration by interfering with VEGF-stimulated NO release. *Int J Biochem Cell Biol* 2008; 40: 2120-2128.
37. Sulochana KN, Fan H, Jois S, *et al.* Peptides derived from human decorin leucine-rich repeat 5 inhibit angiogenesis. *J Biol Chem* 2005; 280: 27935-27948.
38. Reed CC, Waterhouse A, Kirby S, *et al.* Decorin prevents metastatic spreading of breast cancer. *Oncogene* 2005; 24: 1104-1110.
39. Czekierdowski A, Czekierdowska S, Danilos J, *et al.* Microvessel density and CpG island methylation of the THBS2 gene in malignant ovarian tumors. *J Physiol Pharmacol* 2008; 59(Suppl 4): 53-65.
40. Czekierdowski A, Czekierdowska S, Czuba B, *et al.* Microvessel density assessment in benign and malignant endometrial changes. *J Physiol Pharmacol* 2008; 59(Suppl 4): 45-51.
41. Lebelt A, Dzieciol J, Guzinska-Ustymowicz K, Lemancewicz D, Zimnoch L, Czykier E. Angiogenesis in gliomas. *Folia Histochem Cytobiol* 2008; 46: 69-72.
42. Jarvelainen H, Puolakkainen P, Pakkanen S, *et al.* A role for decorin in cutaneous wound healing and angiogenesis. *Wound Repair Regen* 2006; 14: 443-452.
43. Schonherr E, Sunderkotter C, Schaefer L, *et al.* Decorin deficiency leads to impaired angiogenesis in injured mouse cornea. *J Vasc Res* 2004; 41: 499-508.
44. Schonherr E, Levkau B, Schaefer L, Kresse H, Walsh K. Decorin affects endothelial cells by Akt-dependent and -independent pathways. *Ann N Y Acad Sci* 2002; 973: 149-152.
45. Fiedler LR, Schonherr E, Waddington R, *et al.* Decorin regulates endothelial cell motility on collagen I through activation of insulin-like growth factor I receptor and modulation of alpha2beta1 integrin activity. *J Biol Chem* 2008; 283: 17406-17415.
46. Nelimarkka L, Salminen H, Kuopio T, *et al.* Decorin is produced by capillary endothelial cells in inflammation-associated angiogenesis. *Am J Pathol* 2001; 158(2): 345-353.
47. Ramont L, Brassart-Pasco S, Thevenard J, *et al.* The NC1 domain of type XIX collagen inhibits in vivo melanoma growth. *Mol Cancer Ther* 2007; 6: 506-514.

Received: August 5, 2009
Accepted: September 10, 2009

Author's address: Dr. Stephane Brezillon, Laboratoire de Biochimie Medicale et Biologie Moleculaire, CNRS UMR 6237, Faculte de Medecine, F51095 Reims Cedex, France; Phone: +33-326-913532; Fax. +33-326-918055; E-mail: stephane.brezillon@univ-reims.fr